Self-sustaining Hybrid Renewable Energy DC Micro Grid System with Ideal Energy Superintendence for AC Load Operation

Gughapriyan D. [1], Abinesh P.

[1] Site Engineer, Bharat Enterprises
India

Published in IJIRMPS (E-ISSN: 2349-7300), Volume 10, Issue 6, November-December 2022

Abstract
The paper presents a proposed design of SEPIC with high voltage gain for sustainable energy applications. The suggested circuit is structured by combining the standard SEPIC with a magnifying module. Hence the converter profits from various assets that the specific converter has, like uninterrupted input current. Also, high voltage gain and input current continuity makes the proposed converter applicable for sustainable energy sources. The altered SEPIC converter (MSC) gives higher voltage gain compared to standard SEPIC and recently addressed converters with single-controlled switch. The analysis of voltage gain in continuous current mode (CCM) and discontinuous current mode (DCM) is carried out by considering the non-idealities of semiconductor devices and passive components. The preference of semiconductor devices depending on voltage- current rating is put forward along with the designing of reactive components. The numerical simulation and experimental work is done and the results demonstrate viability of the MSC concept and theoretical analysis.

Keywords: Capacitors, SEPIC Converter, DC-DC Converter, Ideal Energy, DCM, CCM

List of Abbreviations

Sr. No.	Abbreviations	Expansion
1	SEPIC	Single Ended Primary Inductor Converter
2	MSC	Modified SEPIC Converter
3	CCM	Continuous Conduction Mode
4	DCM	Discontinuous Conduction Mode
5	RES	Renewable Energy Sources
6	HFT	High Frequency Transformer

Introduction

The utilization of fossil fuels has tremendously increased in the last decade, which leads to environmental contaminations and increases the cost of the system [1]. These problems attracts the researcher to work on Renewable Energy Resources (RES) such as Photovoltaic (PV), wind turbine, fuel cells, etc. Among these RES, PV is gaining more attraction and become noticeable as consequence of its various advantages such as eco-friendly, abundant in nature, freely available, etc. However, the voltage generated from the PV modules is comparatively low and depends on the environmental conditions [2]. Therefore, in order to boost the PV voltage, series and parallel combinations of PV panels can be a solution to fulfill the load demand, which results in lower efficiency, high cost and large the size of the system [3, 4]. A high voltage gain DC-DC converter can be a practicable solution to boost the low voltage generated from PV. Figure 1 shows the general architecture of modern smart DC grid system integrated with PV and fuel cell system.

To meet the high voltage demand of DC home, electric vehicle, DC microgrid etc. high voltage gain converter is utilized as intermediate stage. The conventional boost, buck-boost, SEPIC, CUK, etc. can be utilized for high voltage applications at maximum duty ratio, but that decreases the efficiency and affects the functionality of converter [5, 6]. Recently, various high voltage gain DC-DC converters have been proposed with utilization of reactive components in boosting stages [7, 8]. In isolated DC-DC converter, High-Frequency Transformer (HFT) adopted to boost the input voltage by adjusting its turn ratio [9, 10]. Nevertheless, voltage based isolated DC-DC converters have high ripple in the input current and high voltage stress across the secondary side. Moreover, the leakage energy, bulky transformer and multistage power conversion process are the main short-coming of the isolated converters [11]. Besides that, non-isolated DC-DC converters are the impeccable solution for PV application with high efficiency and compact size. In literature, various voltage-boosting techniques such as cascading of converters e.g. Quadratic Boost Converter (QBC) [12], voltage lift structure [13–19] or coupled inductor [20–22] have adopted with non-isolated converter to achieve high output voltage.

In the coupled inductor-based converters, the output is controlled by adjusting turns ratio of inductor coil. The leak- age inductance of the coupled inductor is inexorable which generates a spike in switch current and demands the clamping circuit to suppress the current spike [23]. By utilizing the volt- age lifting techniques/structures, numerous high gain DC-DC converters have been proposed in [9, 19]. In [24], second order boost converter with voltage multiplier has been dis- cussed. Presented converter has flexible structure and output voltage depends on the duty ratio as well as on the number of voltage multiplier level. Nonetheless, converter has low voltage gain even though with several numbers of voltage multiplier levels. Additionally, Converter has very high input current ripple in the proportion of average input current that implies high-value inductor. In addition, converter has balancing issue of the voltage multiplying capacitors.

Moreover, efficiency is decreasing with increasing number of levels by the effect of the uncontrolled diodes. A switched capacitor based high gain DC-DC converter with multiple inductors and capacitors has been present in [24]. The presented converter shows the good regulation with lower voltage gain in comparison to the number of components. In [11], high gain switched capacitor DC-DC converter with the active network has been presented. The converter achieves high gain with pulsating current and poor regulation. The converter controlled with two switches and that make the complexity in the control scheme and affects the efficiency. Additionally, dis- continues input current is another drawback of the circuitry which proves the minimum utilization of the sources [25].

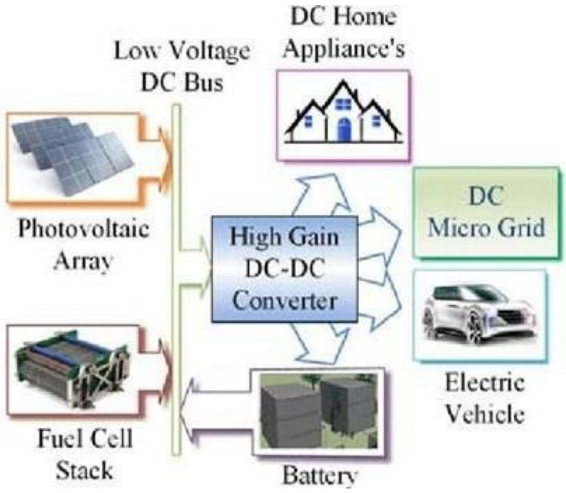

Figure 1: Modern Smart Grid Architecture

Literature Survey

Title 1: Bidirectional Power Flow Control in a DC Microgrid Through a Switched-Capacitor Cell Hybrid DC–DC Converter
Authors: O. Cornea, G.-D. Andreescu, N. Muntean, and D. Hulea,
Year: 2017
Description: This paper focuses on a bidirectional hybrid DC-DC Converter suitable as an interface between two dc voltage buses in various applications including micro grids. The switched-capacitor cell, incorporated in the Converter topology, gives the advantage of high voltage conversion ratio without using a transformer. This paper analyses the converter operation and the stability in the step-up and step-down operating modes through the state-space averaging method and through the pulse width modulation switch model method applied on an equivalent circuit model. Experimental results obtained from a 2 kW Converter prototype confirm the theoretical considerations and the simulation results.

Title 2: Power electronics—The key technology for renewable energy system integration
Authors F. Blaabjerg, Y. Yang, K. Ma, and X. Wang
Year: 2015
Description: In order to realize the transition smoothly and effectively, Energy conversion systems, currently based on power electronics technology, will again play an essential role in this energy paradigm shift. Using highly efficient power electronics in power generation, power transmission/distribution and end-user application, together with advanced control solutions makes the way for renewable energies. In light of this, some of the most emerging renewable energies, eg. Wind energy and Photovoltaic, which by means of Power Electronics are changing character as a major part in the Electricity generation, are explored in this presentation.

Title 3: High-Efficiency Isolated Boost DC–DC Converter for High-Power Low-Voltage Fuel-Cell Applications
Authors: M. Nymand and M.A.E. Andersen
Year: 2010
Description: A new design approach achieving very high conversion efficiency in low-voltage high-power isolated boost dc-dc converters is presented. The transformer eddy-current and proximity effects are analyzed, demonstrating that an extensive interleaving of primary and secondary windings is needed to avoid high winding losses. Detailed test results from a 1.5-kW full-bridge boost dc-dc converter

verify the theoretical analysis and demonstrate very high conversion efficiency. The efficiency at minimum input voltage and maximum power is 96.8%. The maximum efficiency of the proposed converter is 98%.

Title 4: Isolated step-up converter based on flyback converter and charge pumps
Authors: I. Hwu and W.Z. Jiang
Year: 2014
Description: In this study, a single switch isolated Step-up Converter is presented, which is derived from the traditional Flyback Converter and charge pump concept. The proposed Converter possesses an output inductor, so the output current is non-pulsating. Moreover, there are several advantages of the proposed converter over the traditional Flyback Converter, such as higher voltage conversion ratio with only additional four passive elements, and smaller voltage and current ripples, except the same switch voltage stress. In this study, some experimental results are provided to verify the effectiveness of the proposed converter.

Title 5: A single-switch quadratic buck–boost converter with continuous input port current and continuous output port current
Authors: N. Zhang, G. Zhang, K.W. See, and B. Zhang
Year: 2017
Description: A single-switch quadratic buck-boost converter with continuous input port current and continuous output port current is proposed in this paper. Compared with the traditional buck-boost converter, the proposed converter can obtain a wider range of the voltage conversion ratio with the same duty cycle.

3. Modified SEPIC Converter

In this paper, a proposed structure of single switch non-isolated high gain SEPIC is introduced for high voltage application. The MSC has single input-output port and derived by transforming the classical SEPIC as shown in Figure 2(a). Figure 2(b) shows the power circuit of MSC consisting three inductors (LX, LY and LZ), three capacitors (C1, C2 and C3) and three diodes (D1, D2 and D3) which are controlled by single switch S with switching frequency (fs). In the MSC, inductor LY and Capacitor C1 serve as a voltage-boosting element in addition with two diodes. The key features of the proposed MSC are: (1) operates with single switch that reduces the complexity of control circuitry, (2) continuous input current, (3) high voltage gain, (4) maximum utilization of input source.

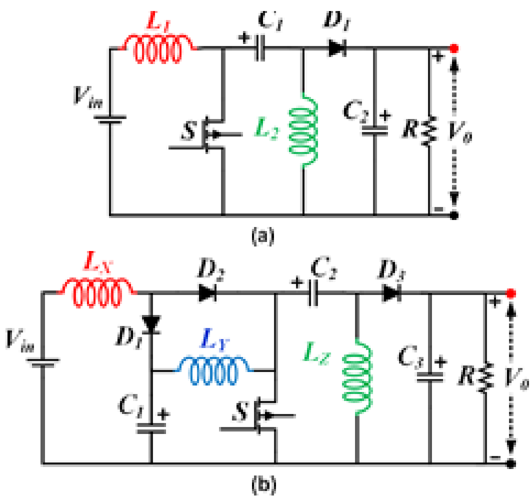

Figure 3: Power Circuitry of (a) SEPIC, and (b) MSC, CCM Operating Modes of MSC

4. CCM Operation and Analysis

In order to explain the steady state operation, some assumptions are to be consider as: all components to be ideal and all capacitors should be large enough to achieve constant voltage. The MSC controlled by single switch S, hence the converter operates in two different modes as mode-I (t0 to t1) and mode-II (t1 to t2) as shown in Figure 4(c) and 4(d) respectively. Where k is duty ratio and TS 1/FS is the time required to complete one switching operation.

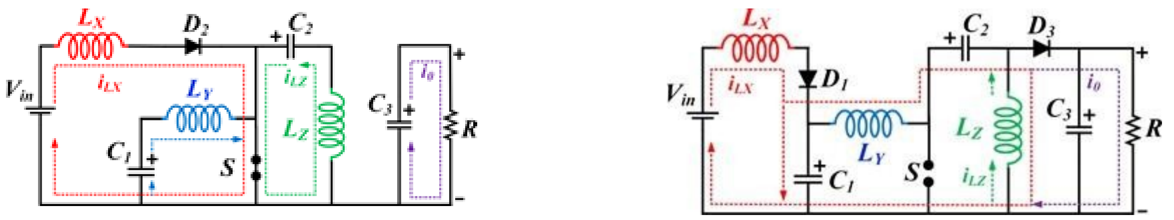

(c) (d)

Figure 4.1: (c) mode-I, and (d) mode-II

Mode One Operation

In mode-I, three inductors are magnetized with current path as follow: inductor LX from input supply (Vin − VLX − D2 − S − Vin), inductor LY from capacitor C1 (VC1 − VLY − S − VC1) and inductor LZ from capacitor C2 (VC2 − S − VLZ − VC2). At the same instant, capacitor C3 reverse bias the diode D3 and transfer energy to the load as shown in Figure 2(c). The characteristic waveforms of each component in mode-I are presented in Figure 4.2.

VLX = Vin
VLY = VC1 mode-I (1)
VLZ = VC2

Where, VLX, VLY, VLZ are the voltages across inductor LX, LY, LZ respectively. VC1, VC1 are the voltage across capacitor C1, C2 respectively.

Mode T5WO Operation

In mode-II, all three inductors are demagnetized as follow: inductor LX along with input voltage (Vin) charges the capacitor C1 (Vin − VLX − D1 − C1 − Vin). The combination of inductor LY and capacitor C1 charges to capacitor C2 through the path VC1 VLY VC2 D3 V0 VC1. Also at the same time, inductor LZ discharges through the load with following the path (VLZ D3 V0) as shown in Figure 2(d). The characteristic waveforms of each component in mode-II.

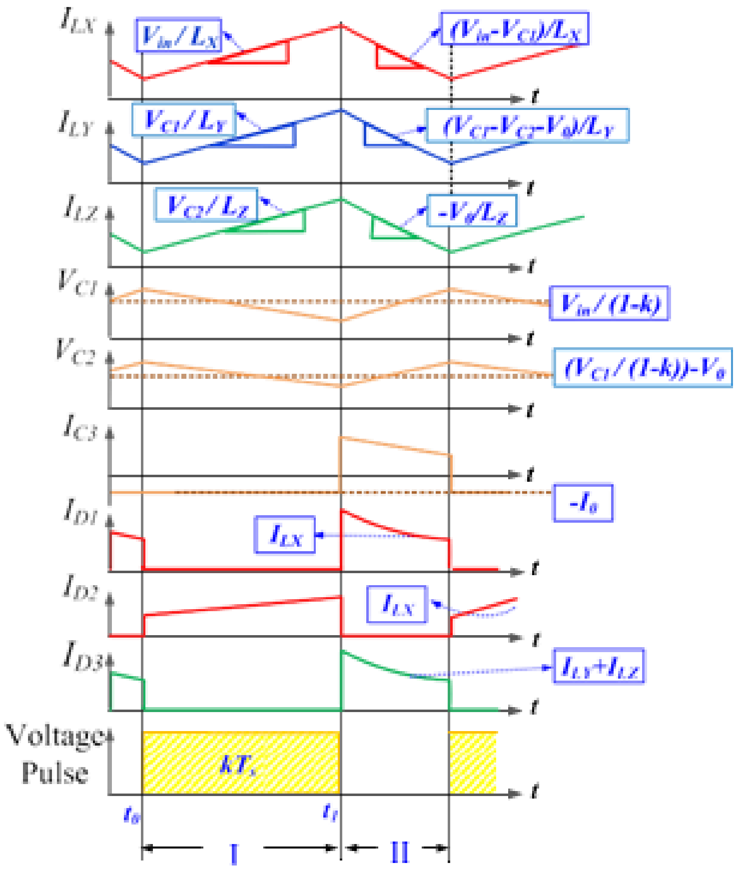

Figure 4.2: Characteristic Waveforms of MSC in CCM

VLX = Vin − VC1

VLY = Vin − VL1 − VC2 − V0 mode-II (2)

VLY = VC1 − VC2 − V0 VLZ = V0

Where, VC0 is the voltage across capacitor C3. By applying Inductor Volt Second Balance (IVSB) principle for the inductors LX , LY and LZ.

$$\frac{VC1}{Vin} = \frac{1}{1-k} \quad (3)$$

Vc2 = Vc1 – Vo (4)

$$\frac{Vo}{Vc1} = \frac{k}{1-k} \quad (5)$$

$$MCCM = \frac{Vo}{Vin} = \frac{k}{(1-k)^2} \quad (6)$$

Equation (6) represents the voltage gain of the proposed converter in CCM mode.

5. DCM Operation and Analysis

The MSC can be operates in Discontinuous Conduction Mode (DCM) as current through inductor/s reaches to zero levels individually or together as respective diode become reverse bias. The DCM operation of MSC is divided into three modes as mode-I, mode-II and mode-III. Where, mode-I and mode-II have similar operating principle similar to CCM. Whereas current and respective diode operating state, the MSC can be work in three different possible DCM mode as mode-A, mode-B and mode-C. In mode-A, inductor LX current (ILX)min individually reach to zero level as diode D1 becomes reverse bias. In mode-B, diode D1 is forward bias and Diode D3 becomes reverse bias due to inductor LY and LZ current ((ILY)min, (ILZ)min). Similarly in mode-C, both diodes D1 and D3 become reverse bias by the effect of current through inductor LX, LY and LZ. The power circuitry with respective current path in three possible DCM modes are shown in Figure 4. Based on the three different possible modes, MSC has three different voltage gain in DCM. Hence, for simplicity the MSC is analyzed with mode-B DCM mode. The respective characteristic waveforms of each component are shown in Figure 5.1.

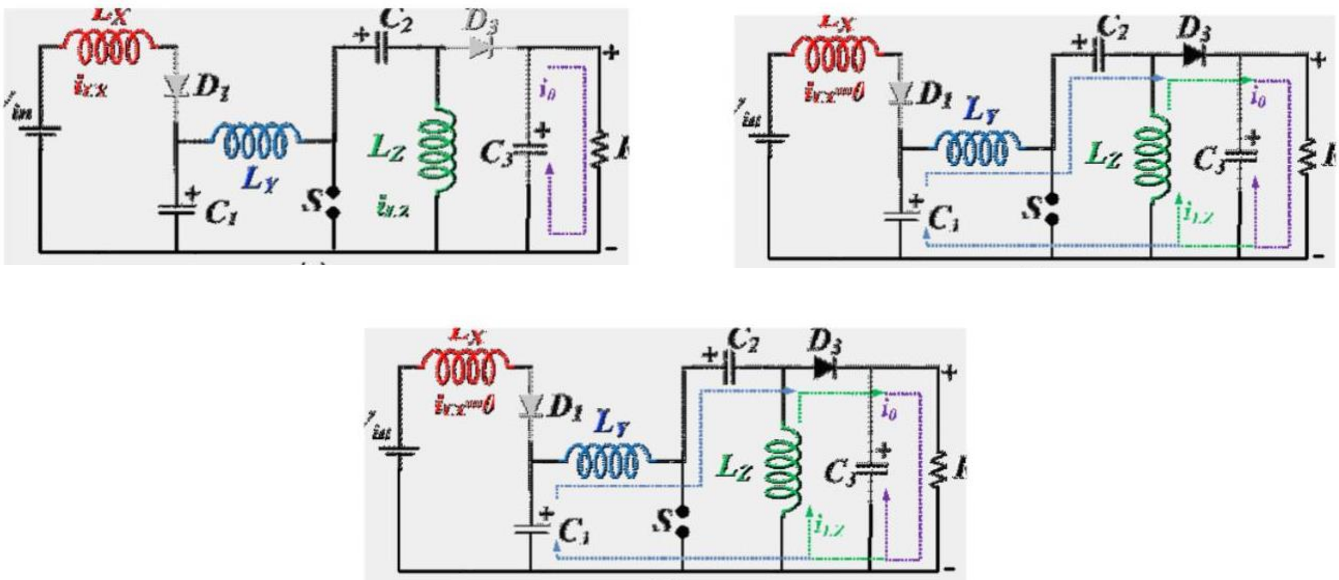

Figure 5.1: Possible DCM Operating Modes of MSC (a) mode-A, (b) mode-B, and (c) mode-C

In mode 1, switches S turned ON. For this mode, the peak amplitude of current through inductor LX, LY and LZ can be expressed as:

(ILY)max = VC1kTSMODE 1

During continuous conduction mode, the inductor current in the energy transfer never reaches zero value. In the case of the discontinuous conduction mode, the inductor current falls to zero level which is very common in DC-to-DC converters.

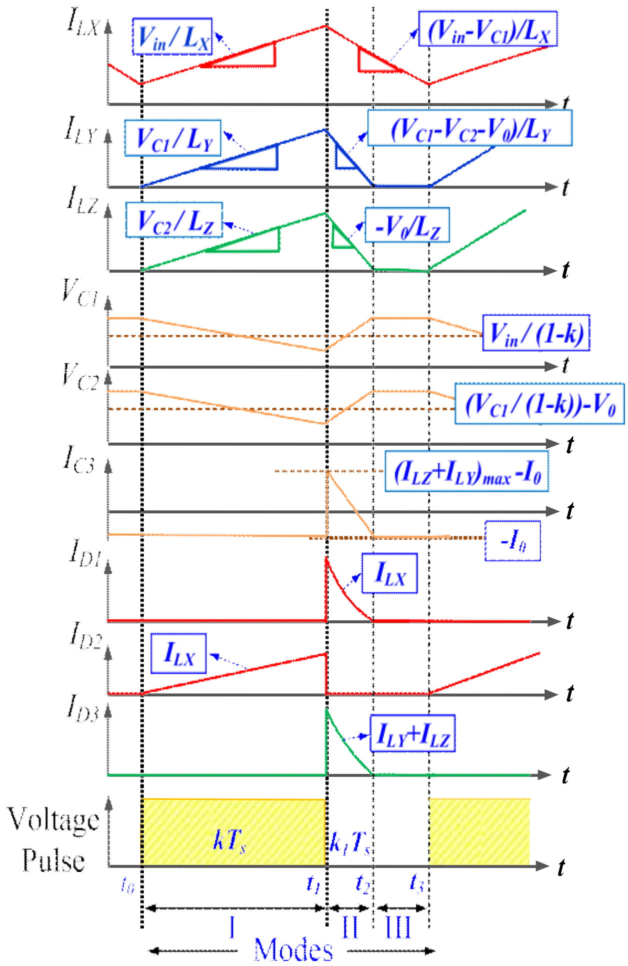

Figure 5.2: Characteristic Waveforms of MSC in mode-B of DCM

The Figure 5.2 shows Characteristic waveforms of MSC in mode-B of DCM. In mode 2, switches S turned OFF. For this mode, the peak amplitude of current through inductor LX, LY and LZ can be expressed as:

(ILZ)min = V0k1TS

The equivalent circuit of mode-III (mode-B) shown in Figure 4(b). In this mode, switches S turned OFF. At the end of this mode, the energies stored in inductor LY and LZ are zero. Hence, only energy stored in capacitor C3 is discharges to the load.

k1 = VC1kV0

The boundary for CCM and DCM is derived as τB = (1 − k)2

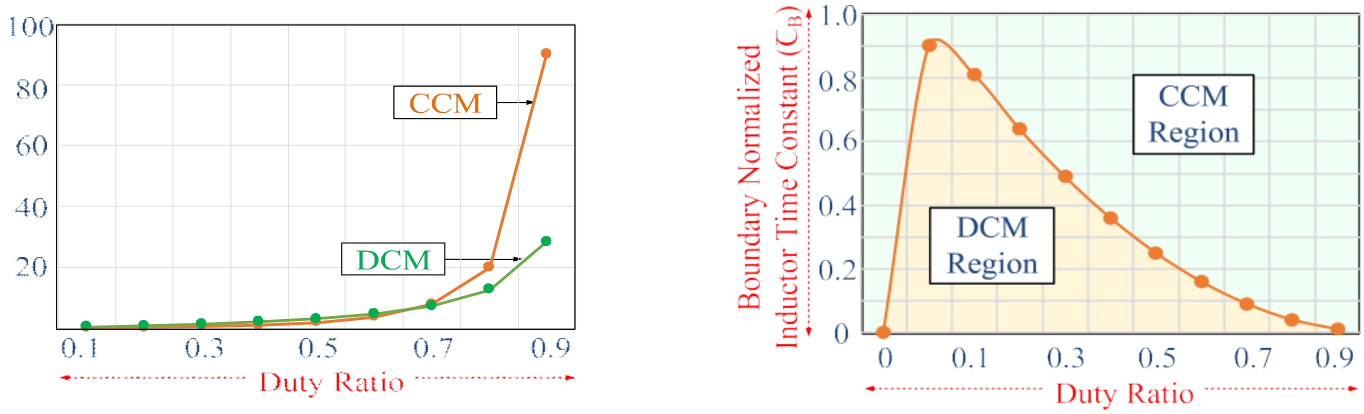

Figure 5.3: (a) Plot of Voltage Gain of MSC in CCM and DCM vs. Duty Ratio, and (b) Plot of Boundary Normalized Inductor Time Constant vs. Duty Ratio

The plot of voltage gain of MSC in CCM and DCM mode Vs. duty ratio is depicted in Figure 5.3 (a). Figure 5.3 (b) represents the graph of boundary normalized inductor time constant vs. duty ratio. It is noteworthy that, if τ is greater than τB, then MSC operates in CCM. It is investigated that, after attaining the peak value there is decrement in normalized inductor time constant (τB) when duty ratio k is increased.

6. Design Consideration of Inductors

The selection of inductor depends on the duty ratio, switching frequency and resistive load [3]. The current carrying capacity and critical value of respective inductor to operate MSC in CCM is derived by:

$$L(z)CRIT = \frac{(1-k)R}{2fS}$$

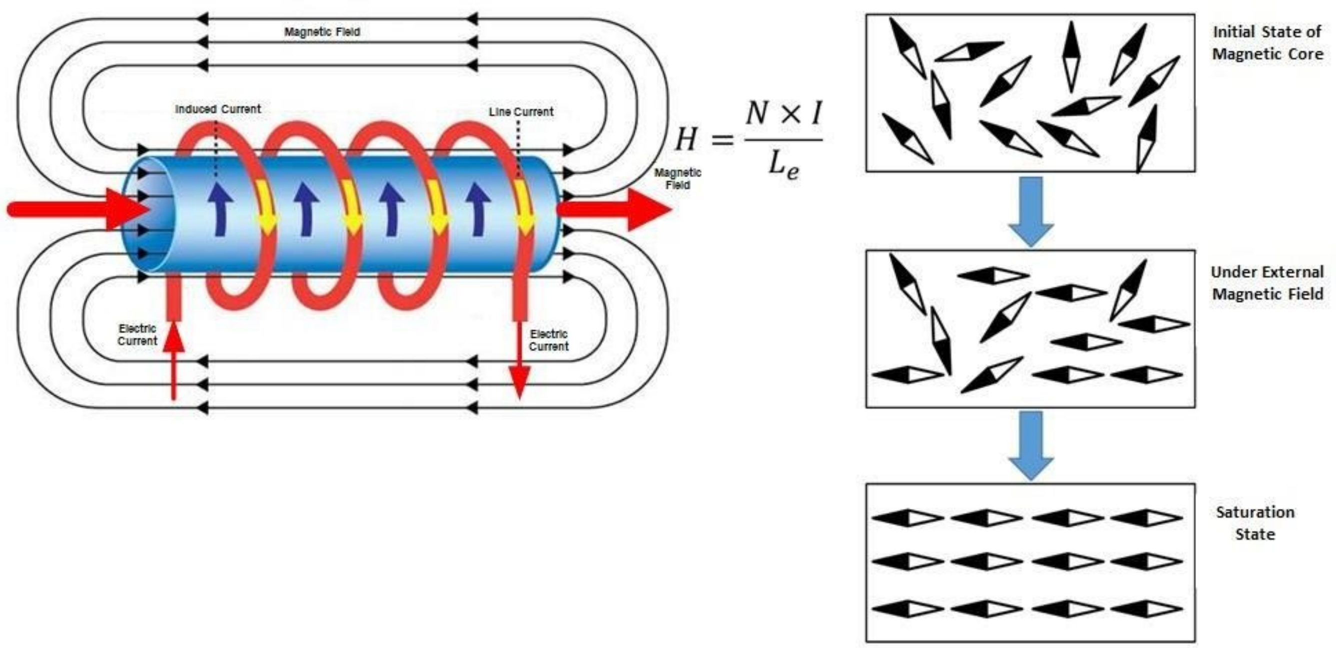

Figure 6.1: Inductor Coil

6.1. Factors Affecting Inductance

Rated Current

Since inductors are constructed of coiled wire, and any wire will be limited in its current-carrying capacity by its resistance and ability to dissipate heat, you must pay attention to the maximum current allowed through an inductor. Since inductor wire has some resistance, and circuit design constraints typically demand the inductor be built to the smallest possible dimensions, there is no such thing as a “perfect” inductor. Inductor coil wire usually presents a substantial amount of series resistance, and the close spacing of wire from one coil turn to another (separated by insulation) may present measurable amounts of stray capacitance to interact with its purely inductive characteristics.

Unlike capacitors, which are relatively easy to manufacture with negligible stray effects, inductors are difficult to find in “pure” form. In certain applications, these undesirable characteristics may present significant engineering problems.

Inductor Size

Inductors tend to be much larger, physically, than capacitors are for storing equivalent amounts of energy. This is especially true considering the recent advances in electrolytic capacitor technology, allowing incredibly large capacitance values to be packed into a small package. If a circuit designer needs to store a large amount of energy in a small volume and has the freedom to choose either of capacitors or inductors for the task, he or she will most likely choose a capacitor.

A notable exception to this rule is in applications requiring huge amounts of either capacitance or inductance to store electrical energy: inductors made of superconducting wire (zero resistance) are more practical to build and safely operate than capacitors of equivalent value, and are probably smaller too.

Interference

Inductors may affect nearby components on a circuit board with their magnetic fields, which can extend significant distances beyond the inductor. This is especially true if there are other inductors nearby on the circuit board. If the magnetic field or more inductors are able to “link” with each other turns of wire, there will be Mutual inductance present in the circuit as well as self-inductance, which could very well cause unwanted effects.

This is another reason why circuit designers tend to choose capacitors over inductors to perform similar tasks: capacitors inherently contain their respective electric fields neatly within the component package and therefore do not typically generate any “mutual” effects with other components.

7. Design Consideration of Capacitors

The value of capacitors depends on the voltage ripple (OVC1in C1, OVC2 in C2 and OVC3in C3), duty ratio, load resistance, and switching frequency [3]. All three capacitors C1, C2 and C3 are selected with following expression as:

I Σ = O LY = in + in LY + 2 (1 − k) 3R2 (1 − k) LYfs

Capacitor Working Voltage

Working Voltage: Since capacitors are nothing more than two conductors separated by an insulator (the dielectric), you must pay attention to the maximum voltage allowed across it. If too much voltage is applied, the "breakdown" rating of the dielectric material may be exceeded, resulting in the capacitor internally short-circuiting.

Capacitor Polarity

Polarity: Some capacitors are manufactured so they can only tolerate applied voltage in one polarity but not the other. This is due to their construction: the dielectric is a microscopically thin layer of insulation deposited on one of the plates by a DC voltage during manufacture. These are called electrolytic capacitors, and their polarity is clearly marked.

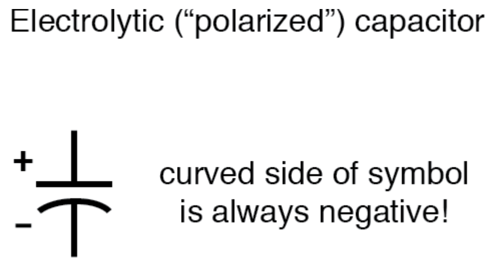

Figure 7.1: Polarizes Capacitor

Reversing voltage polarity to an electrolytic capacitor may result in the destruction of that super-thin dielectric layer, thus ruining the device. However, the thinness of that dielectric permits extremely high values of capacitance in relatively small package size. For the same reason, electrolytic capacitors tend to be low in voltage rating as compared with other types of a capacitor construction.

Capacitor Equivalent Circuit

Equivalent Circuit: Since the plates in a capacitor have some resistance, and since no dielectric is a perfect insulator, there is no such thing as a "perfect" capacitor. In real life, a capacitor has both a series resistance and a parallel (leakage) resistance interacting with its purely capacitive characteristics:

Fortunately, it is relatively easy to manufacture capacitors with very small series resistances and very high leakage resistances!

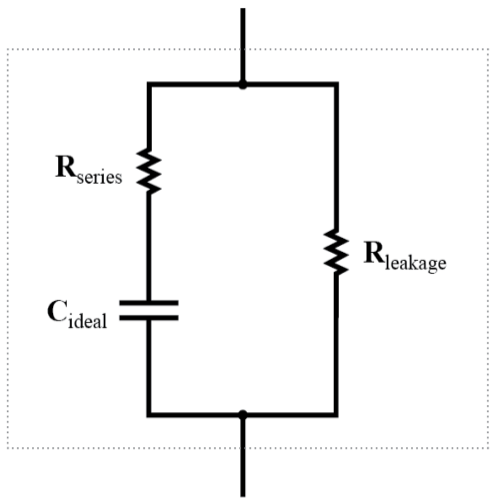

Figure 7.2: Capacitor Equivalent Circuit

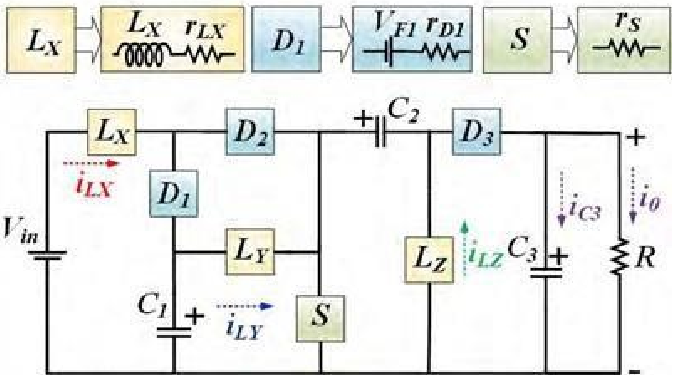

Figure 7.3: MSC with ESR of Inductor, Switch and Voltage Drop of Diodes

8. Efficiency Analysis and Comparison

8.1. Efficiency Analysis

In this sub-section, converter efficiency analysis is discussed. The equivalent circuit of MSC with non-idealities of circuit components i.e. internal resistance of respective components is shown in Figure 7. Where rLX, rLY, rLZ are the Equivalent Series Resistance (ESR) of inductor LX, LY and LZ respectively. Similarly rD1, rD2, rD3 are internal resistance and VF 1, VF 2, VF 3 are the forward voltage drop of three diodes D1, D2 and D3 respectively. Whereas, rS is forward ON state resistance of a controlled switch S The equivalent voltage equations of three inductors with consideration of non-idealities in conducting and non-conducting state are:

$$VLX = Vin - iLX\left(rLX + rS + rD2\right)$$

The below equation gives the relation of output power with the efficiency. To evaluate the power losses and efficiency of MS converter, the losses can be calculated as for each component:

$$\eta = \frac{Po}{Po + PLoss} = \frac{Po}{P + PsLoss + PdLoss + PlLoss + PcLoss}$$

The power loss by each diode can be calculated as:

$$P^{D}\text{ loss} = \frac{Vin\,k\left(1 - k + k2\right)}{R\left(1 - k\right)}$$

The power loss by the capacitors and inductors can be derived as:

$$P^{C}\text{ loss} = rC^{2}\,C_{rms}$$

$$P^{L}\text{ loss} = rL^{2}\,C_{rms}$$

Where, rC is ESR of capacitor. In this paper, magnetic loss by inductor and body diode conduction loss in switches are not considered.

8.2. Comparison with Recently Addressed Converters

The proposed MSC is compared with recently addressed high gain converters as discussed in the literature. The comparison is made in term of number of active and passive components requirements, voltage stress across controlled switch (VDS), voltage gain (MCCM) as tabulated in Table 1. It is observed that, the MSC required less components as compared to other converters. From Figure 9, it is noticed, the proposed converter gives higher voltage gain as compared to other converters.

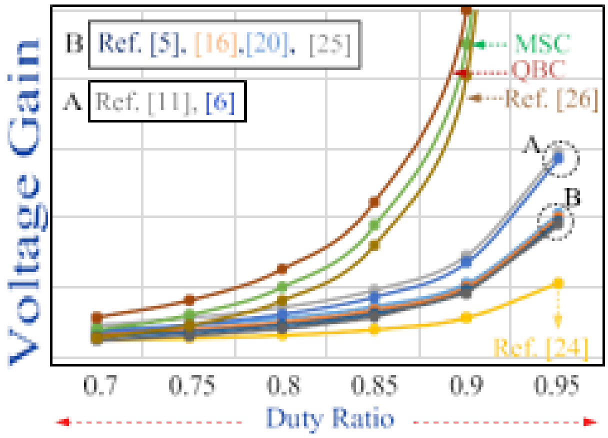

Figure 8.1: Graph of Voltage Gain of Recently Addressed Converter and MSC vs Duty Ratio

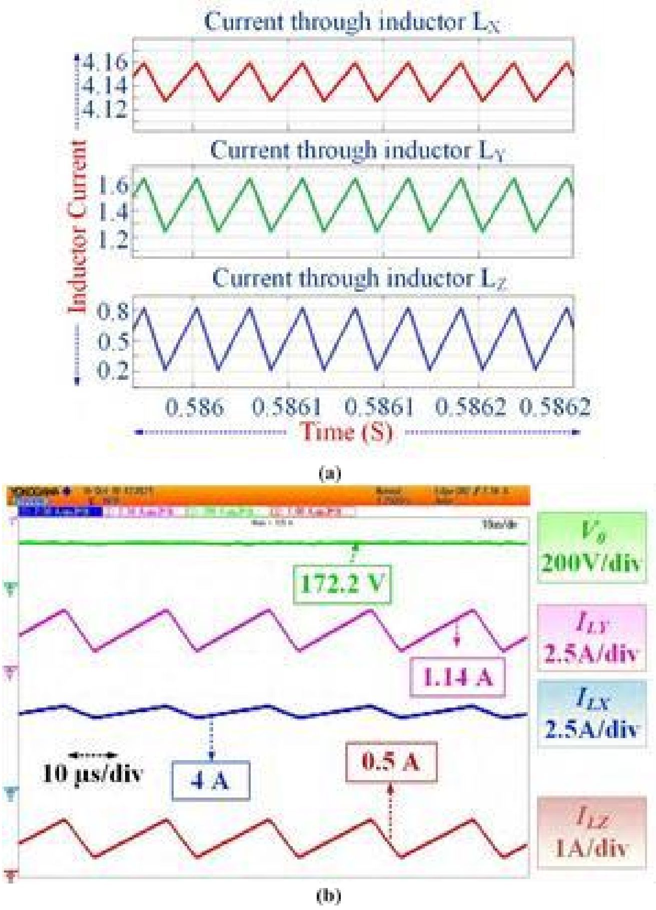

Figure 8.2: Waveform of Current through Inductor LX, LY and LZ in (a) Simulation, and (b) Hardware

9. Simulation Results

Simulation Diagrams

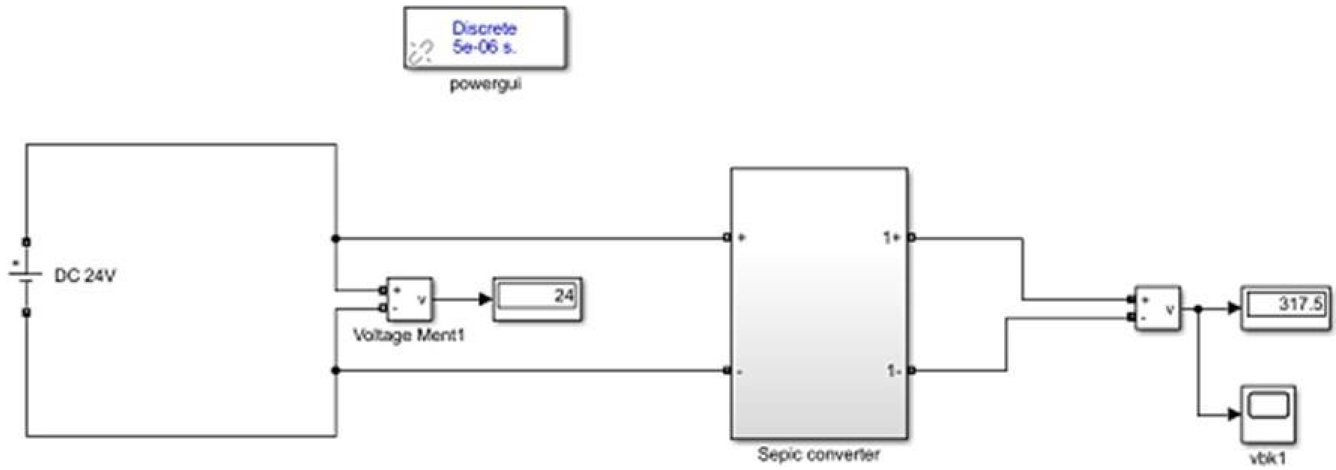

Figure 9.1: MatLab Simulink Model of SEPIC Converter

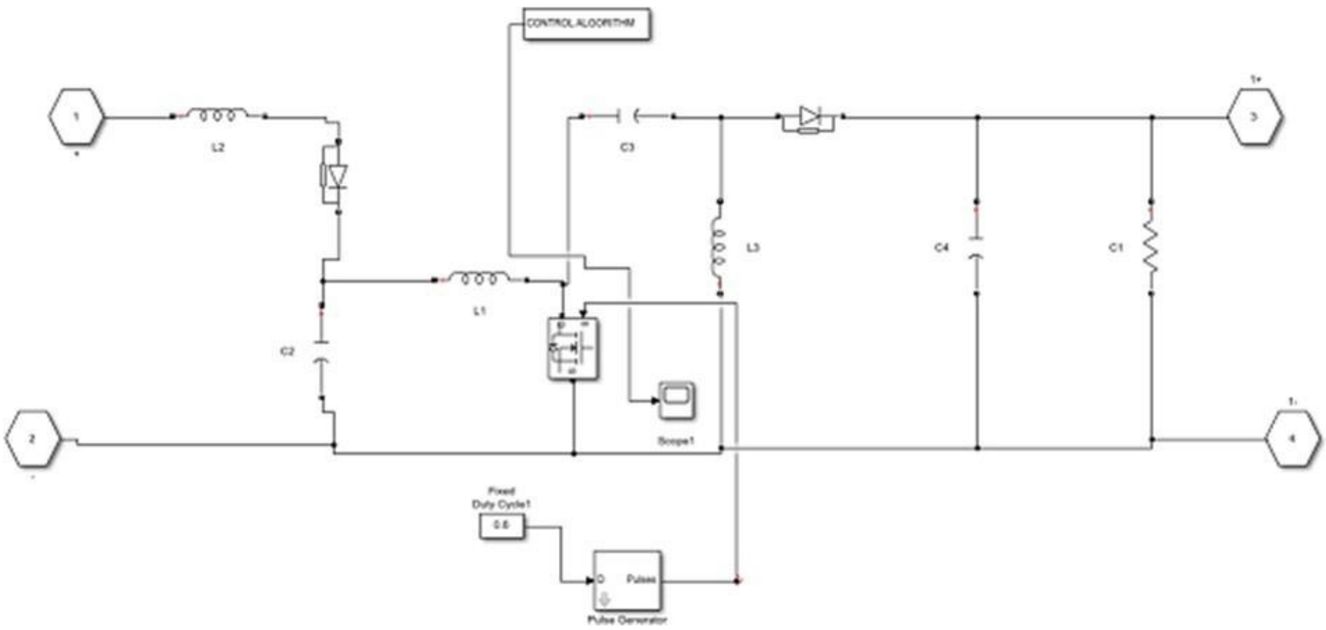

Figure 9.2: SEPIC Converter Sub-system

Simulation Graphs

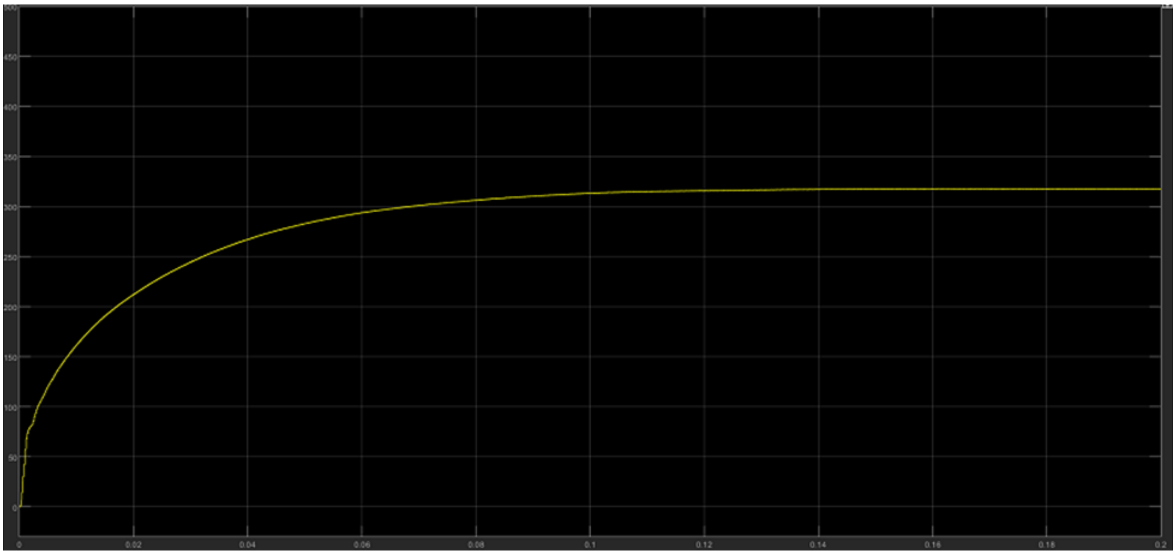

Figure 9.3: Voltage Output

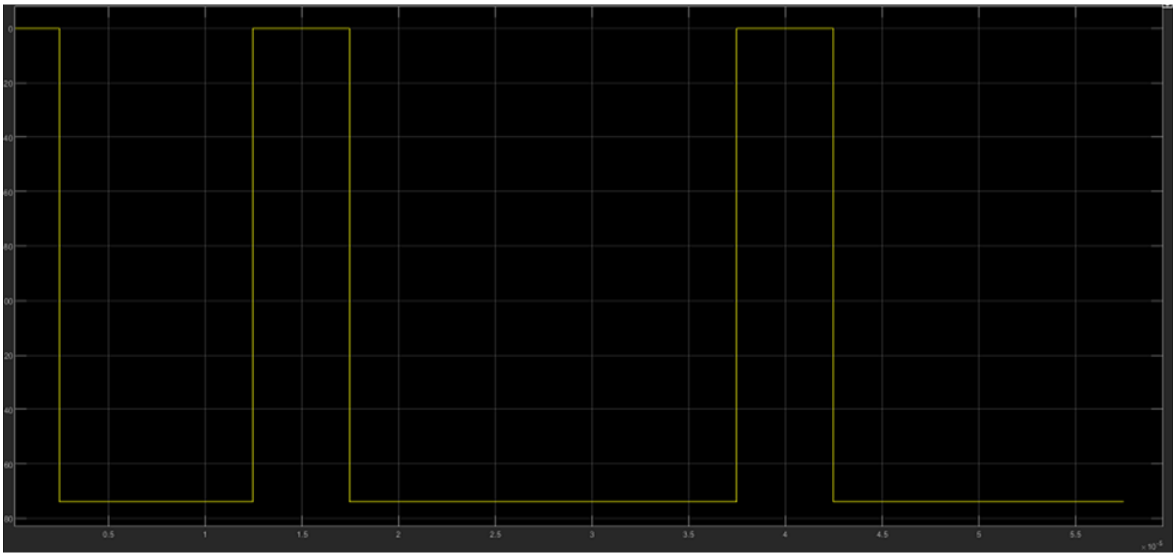

Figure 9.4: Switching Frequency Pulses

The simulation and experimental work of proposed converter is performed to test its functionality. The MSC is implemented according to the aforementioned design procedure with the parameters given in Table 2. To operate the converter in CCM, the inductors LX, LY and LZ values are selected more than respective critical value as derived in (14), (15) and (16), respectively. The gate pulse with 70% duty ratio is generated through Virtex-5 FPGA. Figure depicts the simulation result waveform of inductor LX, LY and LZ current. It is observed that, inductor LX, LY and LZ carry 4 A, 1.4 A and 0.5 A (average) current. Whereas, Figure 9(B) shows the experimental result waveform of output voltage (V0), inductor LY current (ILY), LX (ILX) and LZ (ILZ) current from top to bottom. During mode-I, current through all three inductors are increasing with positive slope at the same instant. Whereas, in mode-II, it starts decreasing with negative slope as expected. Figure 11(a) depicts the simulation results waveform of capacitor C1, C2 and C3 voltage. It is observed that, 80 V is developed across the both capacitor C1 and C2. Also, non-inverted 186 V across the capacitor C3.

Figure 11(b) depicts the experimental waveform of voltage across the capacitor is C2 and C1; current through inductor LX and voltage across capacitor C3 from top to bottom. A non- inverting 76 V, 75.3 V and 172 V is developed across capacitor C1, C2 and C3 respectively in steady state as observed from Figure 11(b). Figure 12(a) and 12(b) shows the blocking voltage across diode D1, D2 and D3 in reverse bias condition. In mode-I, It is observed that Peak Inverse Voltage (PIV) across diode D1 is equal to voltage across capacitor C1 and equal to 76 V. Whereas, PIV across diode D3 is equal to addition of voltage across capacitor C2 and C3 i.e. (VC2 V0 184 V). In mode-II, diode D2 is reverse bias and handle PIV equal to output voltage (V0) and equals to 172 V. The Hardware result waveform of Input voltage (Vin), output current (I0), inductor LX current (ILX) and output voltage (V0) from top to bottom. It is noticed from experimental results MSC operates with 24 V input supply and draw the input current (ILX = I in) of 4 A with input power of 96 W. Furthermore, MSC develop 172 V at the load end (V0) with 0.51 load current (I0).

The DCM operation of proposed converter depends on the inductors value, duty ratio, value of resistive load and switching frequency. Therefore, the DCM mode can be achieved either by decreasing the duty ratio or switching frequency or by increasing the load resistance value. In this paper, the proposed converter operated in DCM operation by decreasing the duty ratio up to 60 % from 70 % without disturbing the other parameters.

The experimental results of proposed converter in DCM mode are shown in the figures. It is observed that, with decrease in duty ratio inductors LX , LY and LZ, current reaches to their maximum level in mode-I. In mode-II, inductors current (ILX ILY and ILZ) start decreasing. Whereas, ILY and ILZ reaches to zero level at the end of mode-II by the effect of reverse bias condition of diode D3. It worth to note that from experimental results as shown in Figure 9(C) and 9(D), the proposed converter work in DCM mode (mode-B) due to the ILZ ILY 0. It is observed that, 92 V is developed at the load end at with 24 V input voltage at inductor time τ 0.142. Whereas, across diode D3 a 152 V (cathode to anode) voltage is appear as PIV.

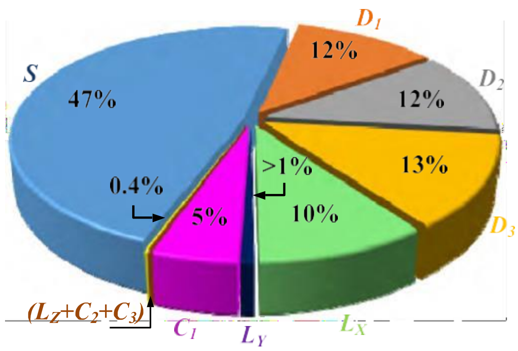

Figure 9.5: Graph of Power Loss Distribution across Each Component with respect to Output Power Loss in (%) at 0.7 Duty Ratio

Efficiency of proposed converter is experimentally analyzed for different power from 60 W to 100 W. It is observed that proposed converter operates with 89.1% efficiency at 60 W load and 91.4% at 100 W. With the help of (37)-(41), the power loss distribution across each component in the proposed converter is calculated with ESR. The power loss distribution across the each components is calculated and graphically shown in Figure 9.5 with respect to output power loss. It is observed that, the maximum power loss is contributed by switch (47%). Whereas, capacitor C2, C3 and inductor LZ have very less contribution (> 1%) in power loss as compared to other components.

10. Conclusion

A new structure of high gain modified SEPIC DC-DC converter has been introduced for renewable energy applications. High voltage gain and continuous input current are the advantages of MSC. The working principle of MSC in CCM and DCM mode has been presented. Additionally, the mathematical voltage gain derivation in CCM and DCM mode with non-idealities consideration and parameter design has been shown sequentially. Also, overall comparison between MSC and other non-isolated single switch converters has been addressed. The performance of the proposed converter is tested with numerical simulation and hardware implementation for 100 W prototype model. The results are shown for 172 V output from 24 V input supply with a gain of almost 8. According to the obtained results, it can be concluded that the proposed converter is well suited for high voltage renewable energy applications.

References

1. F. Blaabjerg, Y. Yang, K. Ma, and X. Wang, “Power electronics—The key technology for renewable energy system integration”, in Proc. Int. Conf. Renew. Energy Res. Appl. (ICRERA), Nov. 2015, pp. 1618–1626.
2. O. Cornea, G.-D. Andreescu, N. Muntean, and D. Hulea, “Bidirectional power flow control in a DC microgrid through a switched-capacitor cell hybrid DC–DC converter”, IEEE Trans. Ind. Electron., vol. 64, no. 4, pp. 3012–3022, Apr. 2017.
3. R.W. Erickson and D. Maksimovic, “Fundamentals of Power Electronics”, 2nd ed. Norwell, MA, USA: Kluwer, 2001.
4. S. Padmanaban, M.S. Bhaskar, P.K. Maroti, F. Blaabjerg, and V. Fedák, “An original transformer and switched-capacitor (T & SC)-based extension for DC-DC boost converter for high-voltage/low-current renewable energy applications: Hardware implementation of a new T & SC boost converter”, Energies, vol. 11, no. 4, p. 783, Apr. 2018.
5. R. Gules, W.M. dos Santos, F.A.F. dos Reis, E.F.R. Romanelli, and A.A. Badin, “A modified SEPIC converter with high static gain for renewable applications”, IEEE Trans. Power Electron., vol. 29, no. 11, pp. 5860–5871, Dec. 2014.
6. M.R. Banaei and S.G. Sani, “Analysis and implementation of a new SEPIC-based single-switch buck–boost DC–DC converter with continuous input current”, IEEE Trans. Power Electron., vol. 33, no. 12, pp. 10317–10325, Jan. 2018.
7. M. Lakshmi and S. Hemamalini, “Non isolated high gain DC–DC converter for DC microgrids”, IEEE Trans. Ind. Electron., vol. 65, no. 2, pp. 1205–1212, Jul. 2018.
8. W. Li and X. He, “Review of non isolated high-step-up DC/DC converters in photovoltaic grid-connected applications”, IEEE Trans. Ind. Electron., vol. 58, no. 4, pp. 1239–1250, May 2011.
9. M. Nymand and M.A.E. Andersen, “High-efficiency isolated boost DC–DC converter for high-power low-voltage fuel-cell applications”, IEEE Trans. Ind. Electron., vol. 57, no. 2, pp. 505–514, Nov. 2010.